The impact of AGN environmental effects on testing general relativity with space-borne gravitational wave detectors

Xiangyu Lyu, Hongyu Chen, En-Kun Li, and Yi-Ming Hu*
MOE Key Laboratory of TianQin Mission, TianQin Research Center for Gravitational Physics & School of Physics and Astronomy, Frontiers Science Center for TianQin, Gravitational Wave Research Center of CNSA, Sun Yat-sen University (Zhuhai Campus), Zhuhai 519082, China

The low-frequency sensitivity of space-borne gravitational-wave detectors such as TianQin offers a new window to test General Relativity by observing the early inspiral phase of stellar-mass binary black holes. A key concern arises if these sBBHs reside in gaseous environments such as active galactic nucleus accretion disks, where environmental effects imprint detectable modulations on the gravitational waveform. Using Bayesian inference on simulated signals containing both environmental perturbations and the dipole deviation, we have assessed the extent to which the presence of environmental effects affects the detectability of dipole radiation. Our results demonstrate that even in the presence of strong environmental coupling, the dipole parameter can be recovered with high precision, and the evidence for dipole radiation remains distinguishable. Crucially, we find that the existence of environmental effects does not fundamentally impede the identification of dipole radiation, provided both effects are simultaneously modeled in the inference process. This study establishes that future tests of modified gravity with space-borne observatories can remain robust even for sources in astrophysically complex environments.

I. INTRODUCTION

The LIGO-Virgo-KAGRA (LVK) collaborations have now reported over two hundred confirmed detections of stellar mass binary black hole (sBBH) systems [1–5]. It provides a unique laboratory for testing the predictions of General Relativity (GR) in the strong field [6–8]. The standard approach in such tests is to search for deviations from the GR-predicted waveform, often parameterized by introducing modifications to the post Newtonian (PN) coefficients that describe the binary's inspiral evolution. These phenomenological tests have been applied across the GW spectrum, from ground-based detectors to space-borne GW detectors like TianQin [9], LISA [10], and Taiji [11] for sBBH systems [12–19]. However, a common and significant limitation in many of these tests is the foundational assumption that the sBBH coalescence occurs in an ideal vacuum environment.

The assumption of a vacuum environment is likely invalid for a distinct subset of sBBHs. Many population analyses have implied that a fraction of the LVK observed sBBH systems may form and merge within dense environments, particularly the gaseous accretion disks of active galactic nucleus (AGN) [20–29]. Especially, for the heavier sBBH systems like GW190521 system [30], Graham et al. [31] have reported the sBBH system could be accompanied by an EM counterpart in an AGN system. If true, these mergers do not occur in vacuum but are embedded in a place where environmental interactions become significant, e.g. physical processes including gas accretion onto the black holes [32], dynamical friction(DF) from the surrounding medium [33, 34], and gravitational acceleration from the central supermassive black hole actively perturb the binary's orbital evolution [35–38].

These astrophysical environmental effects leave a characteristic imprint on the emitted gravitational-wave signal. Specifically, they introduce corrections to the waveform's phase evolution that appear at negative PN orders (e.g., -4PN,-5.5PN), which are most significant during the long, early inspiral phase at low frequencies [39, 40]. Crucially, the sensitive band of future space-borne gravitational-wave detectors like TianQin [9] and LISA [10] is well suited to observe this low-frequency regime. Many researches have confirmed that space-borne observatories could detect and measure these environmental modifications [33, 41–44], whereas ground-based detectors cannot [45].

The detectability of environmental effects with space-borne missions introduces a critical problem for testing fundamental physics. If an sBBH signal is analyzed with a template that assumes a vacuum environment but the source actually resides in an AGN disk. It will lead to a biased inference of modified gravity effects or a misinterpretation of the nature of the observed deviation [40, 46–48].

This paper is organized as follows: In SectionII, we focus on detailing the phenomenological parameterization of the three key AGN environmental effects (gas accretion, dynamical friction, and center-of-mass(CoM) acceleration) and the negative PN order corrections to the GW phase. In SectionIII, we will introduce the response function used for space-borne GW detectors and the sBBH waveform in the frequency domain. In section.IV, we describe the Bayesian inference framework used to extract the information from the observation data, including the use of a heterodyne likelihood method to efficiently analyze the observation data. In Section.V, we present the results of our analysis. We show comprehensive parameter estimation results in the form of corner plots and calculate Bayes factors to quantify TianQin's ability to

*Corresponding author: huyiming@mail.sysu.edu.cn

distinguish the modified gravity effect with the presence of environmental effects. Finally, in Section VI, we summarize our findings regarding the environmental threshold for reliable gravity tests and discuss the implications and prospects for future tests of General Relativity with space-borne gravitational-wave detectors.

II. ENVIRONMENTAL EFFECTS AND MODIFIED GRAVITY

AGN is a promising formation channel of sBBH systems, and it comprises the center supermassive black hole (SMBH) and the surrounding dense gaseous accretion disk. As much gas exists, the AGN disk provides a suitable environment for bonding the individual black holes into the binary systems by the drag from gas gravitation [49, 50] or the close encounters [51]. Furthermore, the high density of the compact objects in the galactic core [52, 53] will increase the formation rate of the sBBH systems. Besides, the existence of the migration traps in AGN disks will also force the individual black hole (BH)s or stellar-mass compact objects to stay in a narrow region, resulting in numerous sBBH systems formation events [54–56].

The GW190521 system [57] has garnered significant attention due to its component black hole (BH) masses, which are located within the pair-instability supernova (PISN) mass gap. This observation challenges the traditional stellar evolution theories [58, 59], as it implies the existence of BHs in a mass range that was previously considered implausible through the stellar evolutionary channels. To address this discrepancy, the scientists promoted the GW190521 system may form in AGN disks [23, 60]. And this hypothesis was further developed that the at least 20% observed LVK sBBH systems may originate from the AGN [24, 25]. If we assume the GW190521 system merger in the AGN disk, certain environmental effects could potentially observed from the gravitational wave (GW) signals.

In our work, we consider three environmental effects: accretion from the surrounding gas, binary system center of mass (CoM) acceleration from the center SMBH, and the dynamical friction (DF) from the surrounding gas. Besides these, there are some particular environmental effects in AGN, which have been analyzed in LISA, such as the Doppler effect from the variation of the distance between the detector and the source, the Shapiro effect that came from the nonvanishing gravitational potential of the third body, the gravitational lensing effect caused by the center SMBH and etc [40]. We primarily focus on the accretion, acceleration, and DF effects similar to Toubiana's work [33] and these environmental effects will leave the observable imprints in the corresponding sBBH signals compared with the vacuum situation. We plan to analyze TianQin's ability to distinguish the environmental effects from the observation data. It is worth noticing that we will include the noise effect, which was not considered either of the previous LISA data analysis works (zero-noise realization) [33, 40].

All three environmental effects are expected to manifest in the GW waveform. Firstly, The GW waveform of a BBH system in a vacuum in the frequency domain under the stationary-phase approximation can be represented as:

$$\tilde{h}(f) \sim A(f) e^{i\tilde{\phi}(f)}, \tag{1}$$

where $\tilde{h}$ is the Fourier transform of the GW strain, $A(f)$ is the amplitude, and $\tilde{\phi}(f)$ is the phase. The presence of an AGN environment could introduce additional features to this waveform, the accretion effect will typically increase the mass of the either component BH in the binary system, leading to deviations from the vacuum scenario. The phase derivation from the accretion [32] can be expressed like:

$$\tilde{\phi}_{\rm accretion} \approx -f_{\rm Edd}(8\xi + 15)\frac{75 M_c}{851968\tau_S}[\pi M_c f(1+z)]^{-13/3}, \tag{2}$$

where $f_{\rm Edd}$ is the Eddington ratio, ξ describes the effect of the momentum transfer from the accreted gas [32], was considered to be zero in this work , $\tau_S = 4.5 \times 10^7$ yr is the Salpeter time, M_c and z is the chirp mass and the redshift of binary system. Besides, the phase derivation from the acceleration of CoM [35, 36, 61] is listed:

$$\tilde{\phi}_{\rm acceleration} \approx \frac{25 M_c}{65536}\dot{v}^{||}(t_c)[\pi M_c f(1+z)]^{-13/3}, \tag{3}$$

the parameter $\dot{v}^{||}(t_c)$ speed acceleration alone the sight line [35]. As shown in Equ.2 and Equ.3, both accretion and acceleration appear at the -4PN, therefore, we include the two environmental effects parameters into a phenomenological PN item $\tilde{\phi}_{-4\rm PN}$ [32, 35, 39, 62] and it represents as $\tilde{\phi}_{-4\rm PN} = \phi_{-4\rm PN}[\pi f M_c(1+z)]^{13/3}$ [63].

Furthermore, the phase derivation from the DF [33] is:

$$\tilde{\phi}_{\rm DF} \simeq -\rho\frac{25\pi(3\eta-1)M_c^2}{739328\eta^2}\gamma_{DF}[\pi f M_c(1+z)]^{-16/3}, \tag{4}$$

where ρ is surrounding gas density, $\eta = \frac{m_1 m_2}{(m_1+m_2)^2}$ is the systematic mass ratio, $\gamma_{\rm DF}$ is the relative DF effect parameter and the definition can be found in Ref.[33].

III. THEORETICAL BASICS

A. sBBH waveform

Since the first reported stellar-mass binary black hole merger event GW150914 in 2016, the ground-based GW detectors have published almost 80 sBBH merger events. These sBBH systems will experience three stages, inspiral, merger, and ringdown and those signals in the frequency domain will also evolve from mili-hertz to hundred-hertz. Thus, the sBBH inspiral-stage signals

could be observed by the space-borne GW detectors, which are well located in mili-hertz sensitive band [13, 64]. In our work, we do not consider the eccentricity and assume the aligned spin for both component BHs.

To describe the inspiral stage sBBHs waveform, we adopted the `IMRPhenomD` waveform [65, 66]. In this waveform model, a sBBH system can be characterized by four intrinsic parameters: two component masses (m_1, m_2) and two component dimensionless spins (χ_1, χ_2); and seven extrinsic parameters: luminosity distance D_L of the source, inclination angle ι that describes the angle between the orbital angular momentum regarding the line of sight, polarization angle ψ, coalescence time and phase (t_c, ϕ_c), the ecliptic longitude and ecliptic latitude (λ, β) in the solar-system barycenter (SSB), and the two more environment effect parameters, $\phi_{-4\mathrm{PN}}$ which related to accretion and acceleration and the gas density ρ_0. We set these parameters as a group that is used for estimation, $\boldsymbol{\theta} = (\chi_a, \chi_l, D_L, M_c, \eta, t_c, \iota, \lambda, \beta, \psi, \phi_c, \phi_{-4\mathrm{PN}}, \rho_0)$, where chirp mass $M_c = \frac{(m_1 m_2)^{3/5}}{(m_1+m_2)^{1/5}}$, systematic mass ratio $\eta = m_1 m_2/(m_1+m_2)^2$. It is worth noticing that we reparametered the spin parameters (χ_1, χ_2) into $\chi_a, \chi_l = (\chi_1+\chi_2)/2, (\chi_1-\chi_2)/2$ to decrease the strong correlation between them and use for parameter estimation.

B. TianQin response

TianQin [9] is a space-borne gravitational wave detector, consisting of three satellites in Earth orbit. Similar with LISA [10] and Taiji [67], TianQin has an equilateral triangle constellation with the armlength of approximately $\sqrt{3} \times 10^5$km. Besides, TianQin's orbital plane is oriented towards the double white dwarf (DWD) system J0806 [68, 69]. And the mission employs a "three month on, three month off" operation modulation to mitigate the thermal load imposed by direct sunlight entering the telescopes.

In this work, we utilize the AET channel [70] to generate response signals of TianQin. These TDI channels are constructed from the delayed signal-link observables y_{slr}, which are expressed as:

$$y_{slr} = \frac{1}{2}\frac{\hat{n}_l \otimes \hat{n}_l}{1-\hat{k}\cdot\hat{n}_l} : \left[h\left(t - L - \hat{k}\cdot\vec{p}_s\right) - h\left(t - \hat{k}\cdot\vec{p}_r\right)\right], \tag{5}$$

In this equation, h represents the transverse-traceless metric perturbation, as detailed in references [71, 72]. L is the armlength of TianQin, $\hat{n}_l$ is the unit vector directed from satellite r to s. Additionally, $\hat{k}$ is the unit vector along the direction of GW propagation, $\vec{p}_r$ and $\vec{p}_s$ represent the positions of the two satellites, respectively.

In our research, we directly generate the response signals in the frequency domain and we start with the single-link observable $\tilde{y}_{slr}$, which is the Fourier transform of y_{slr}. The observable $\tilde{y}_{slr}$ comprises the GW signal $\tilde{h}(f)$ and the transfer function $\mathcal{T}_{slr}$, as given by:

$$\tilde{y}_{slr} = \mathcal{T}_{slr}(f)\tilde{h}(f). \tag{6}$$

Notably, GW signal $\tilde{h}(f)$ indicated in Equ.1 is formulated as $\tilde{h}(f) = A(f)e^{i\tilde{\phi}(f)}$. Furthermore, under the leading-order expansion of the time-frequency relation $t(f) = -\frac{1}{2\pi}\frac{\mathrm{d}\phi(f)}{\mathrm{d}f}$ derived in [73], the transfer function $\mathcal{T}_{slr}$ can be represented as:

$$\mathcal{T}_{slr}(f) = G_{slr}(f, t(f)), \tag{7}$$

$$\begin{aligned} G_{slr}(f,t) =& \frac{\mathrm{i}\pi f L}{2}\mathrm{sinc}[\pi f L(1-\hat{k}\cdot\hat{n}_l)] \\ & \cdot \exp[\mathrm{i}\pi f(L + \hat{k}\cdot(\vec{p}_r+\vec{p}_s))]\ \hat{n}_l \cdot P \cdot \hat{n}_l. \end{aligned} \tag{8}$$

Here, P represents the polarization tensor [74].

IV. DATA ANALYSIS METHODOLOGY

In this work, our objective is to assess the capability of TianQin of testing GR with present of the AGN environment effect in sBBH observation data. And we proceed the whole progress under the primary assumption that the GW signal has been detected, thus concentrating solely on the subsequent data analysis steps, specifically parameter estimation and model selection.

To fulfil these targets, we initially generate the TianQin mock observation data that contains the sBBH signals that are exhibited in the AGN disk. Subsequently, extracting the physical information of the GW signal from this data is essential. For this purpose, we employ Bayesian inference as our methodology.

A. Bayesian inference

The Bayesian inference is widely used in GW data analysis research, and it could extract physical information from the data. In particular, the Bayesian inference allows us to perform PE by providing the probability distribution of the signal's parameters and model selection by evaluating the preference of different physic models given the observation data.

First, we work on the Bayesian inference on PE, and according to the Bayes equation, the posterior probability of the sBBH source parameters $\boldsymbol{\theta}$ can be expressed by:

$$p(\boldsymbol{\theta}|D) = \frac{p(D|\boldsymbol{\theta})\pi(\boldsymbol{\theta})}{p(D)}, \tag{9}$$

D is the observation data, $\pi(D|\theta)$ is the likelihood function, $\pi(\boldsymbol{\theta})$ is the prior information before we obtain the data, and $p(D)$ is evidence or marginal likelihood. In the PE step, since the evidence is a marginalized constant,

the posterior probability will be proportional to the multiplied product of likelihood function $\mathcal{L} = p(D|\boldsymbol{\theta})$ and prior $p(\theta)$:

$$p(\boldsymbol{\theta}|D) \propto \mathcal{L} \times \pi(\boldsymbol{\theta}) \tag{10}$$

In our work, we assume data D to be Gaussian-stationary and the logarithm of the likelihood function $\mathcal{L}$ of the GW signal takes the following form:

$$\ln \mathcal{L} \propto (h(D \mid \boldsymbol{\theta})) - \frac{1}{2}(h(\boldsymbol{\theta}) \mid h(\boldsymbol{\theta})), \tag{11}$$

where $(a \mid b)$ is the inner product between time series $a(t)$ and $b(t)$,

$$(a \mid b) = 4\Re \int_0^{+\infty} \mathrm{d}f \frac{\tilde{a}^*(f)\tilde{b}(f)}{S_n(f)}. \tag{12}$$

$\Re$ is the real part,$S_n(f)$ is the one-side (power spectral density) PSD of the detector noise, $\tilde{a}^*(f)$ is the complex conjugate of $a(t)$.

The sBBH data PE works usually require us to explore the high-dimension parameters space to get the posterior distribution of the GW source's parameters. To fulfil the parameter space exploration, we choose the well-accepted method in GW data analysis, Markov chain Monte Carlo (MCMC). It performs impressively by randomly sampling in high-dimension parameter space and allows the scientists to probe the parameters' posterior distribution with the random sample points' distribution after the convergence. In the PE part, we utilized the python package `emcee` [75] to explore the full parameter space. `emcee` allows users to set multiple walkers to sample the points according to the parameters' posterior value and the parameter's information will be exchanged during the whole sampling procedure, which could improve the efficiency of MCMC sampling [76].

B. Heterodyne likelihood

As mentioned in Subsec.IV A, our approach to exploring the high-dimensional parameter space involves utilizing the MCMC sampling algorithm. The main computational expenses can be divided into two key components: the average calculation time of the likelihood function and the number of sampling steps. Specifically, achieving converged parameter estimation (PE) results typically requires $10^6 \sim 10^7$ likelihood evaluations, as reported in [77, 78]. To expedite this process, many PE studies employ down-sampled waveforms within the likelihood function [74, 78–81], significantly reducing computational overhead under the zero-noise assumption. However, this assumption does not hold in more real data analysis scenarios, necessitating a novel method for noise-inclusive PE.

In our research, we address this challenge by adopting the heterodyne likelihood method, as detailed in [82–84]. Our objective is to perform accurate likelihood calculations with noisy observation data for sBBH signals. As shown in Equ.11 and Equ.12, the logarithm form of the likelihood Ln$\mathcal{L}$ can be expressed by:

$$\mathrm{Ln}\mathcal{L} \propto 4\mathcal{R}\left(\int_0^{+\infty} df \frac{\tilde{D}^*(f)\tilde{h}(f)}{S_n(f)} - \frac{1}{2}\int_0^{\infty} df \frac{|\tilde{h}(f)|^2}{S_n(f)}\right), \tag{13}$$

where $\tilde{h}(f)$ is the Fourier-transform of the GW signal $h(t)$, $\tilde{D}^*(f)$ is the complex conjugate of the observation data in the frequency domain. The core idea of the heterodyne likelihood function is separating the waveform $\tilde{h}(f)$ into a reference waveform $\tilde{h}_0(f)$, which obtains a high likelihood value and slowly changing item $\tilde{r}(f) = \frac{\tilde{h}(f)}{\tilde{h}_0(f)}$. Under the above definition, the two parts of the logarithm likelihood Ln$\mathcal{L}$ can be represented as:

$$(D \mid h) = 4\Re \int_0^{\infty} df \frac{\tilde{D}(f)\,\tilde{h}_0^*(f)}{S_n(f)} \times \tilde{r}(f), \tag{14a}$$

$$(h \mid h) = 4\Re \int_0^{\infty} df \frac{\left|\tilde{h}_0(f)\right|^2}{S_n(f)} \times |\tilde{r}(f)|^2, \tag{14b}$$

In the context of heterodyne likelihood calculation, significant computational efficiencies can be achieved by optimizing the likelihood construction. Firstly, the reference waveform $\tilde{h}_0(f)$, Fourier-transform observation data $\tilde{D}^*(f)$ and noise PSD $S_n(f)$ are only required once and can be stored as constants. Consequently, the $\frac{\tilde{D}(f)\tilde{h}_0^*(f)}{S_n(f)}$ and $\frac{|\tilde{h}_0(f)|^2}{S_n(f)}$ also computed once and stored as a constant during the MCMC sampling process. Secondly, for the remaining slowly varying components: $\tilde{r}(f)$ and $|\tilde{r}(f)|^2$, sampling can be performed on a sparse frequency grid, thereby reducing computational load.

Moreover, the heterodyne likelihood method exhibits substantial computational cost savings and maintains high accuracy. In our practice, compared to the original likelihood function presented in Equation 11, the heterodyne likelihood method reduces the total computational cost by approximately three orders of magnitude. Furthermore, to validate the accuracy of the heterodyne method, we compared the one-dimensional likelihood function of the original likelihood and heterodyne likelihood by fixing all source parameters $\boldsymbol{\theta}$ except a single free parameter θ_i. This comparison was performed over a specific region that contains the true source's parameter value, $\theta_i^{\mathrm{True}} \in [\theta_i^0, \theta_i^1, \cdots \theta_i^n]$, where θ_i^{True} is the true value of the source's parameter θ_i. We tested with all parameters in the sBBH waveform. These results demonstrate that the heterodyne likelihood method accurately approximates the original likelihood function, ensuring both efficiency and precision in scientific data analysis.

C. Savage-Dickey model selection method

To quantitatively assess the evidence for a modified gravity (MG) signature in the presence of confounding environmental effects, we employ Bayesian model selection to compare two competing hypotheses. Specifically, we compute the Bayes factor to evaluate whether the observational data prefer a model that includes both the -1PN dipole term (from MG) and AGN environmental effects ($M_{\rm MG+env}$), or a model that includes only the environmental effects ($M_{\rm env}$). This comparison directly addresses whether the inclusion of the MG parameter is warranted once the environmental contributions are accounted for. The Bayes factor $\mathcal{B}$ in favour of the MG+environment model is defined as the ratio of the marginal likelihoods (evidences):

$$\mathcal{B}^{\rm MG+env}_{\rm env} = \frac{P(D \mid M_{\rm MG+env})}{P(D \mid M_{\rm env})}, \tag{15}$$

where $P(D \mid M) = \int \mathcal{L}(D \mid \boldsymbol{\theta}, M)\pi(\boldsymbol{\theta} \mid M)d\boldsymbol{\theta}$ is the evidence for the model M, with $\mathcal{L}$ denoting the likelihood and π the prior. In practice, we leverage the Savage-Dickey density ratio to compute this Bayes factor efficiently, as $M_{\rm env}$ is nested within $M_{\rm MG+env}$ by setting the dipole amplitude parameter B to zero.

Two different approaches have been wildly utilized in calculating the Bayes factor $\mathcal{B}$: Nested sampling, introduced by Skilling (2006)[85] and the Savage-Dickey method [86], firstly applied in a model selection study of cosmological parameters by Trotta (2005)[87]. While nested sampling provides a principled method for calculating the Bayes factor, it is still computationally intensive and time-consuming, particularly considering the model selection under the high dimensional case. Therefore, the Savage-Dickey ratio, which allows for more efficient computation, is often adopted as an alternative for calculating Bayes factors. It has been widely applied in the cosmology constant analysis [88, 89], isotropic GW background searching in Pulsar Timing Array (PTA) [90], GW searching [91] and PE [92] in the space-borne detector.

The Savage–Dickey ratio simplifies the Bayes factor when a simpler model is nested within a more complex one and the priors of different parameters are separable. In our research, the vacuum model $M_{\rm vac}$ is a special case of the environment model $M_{\rm env}$, where all environmental parameters are set to zero: $\tilde{\phi}_{-4\rm PN} = 0, \tilde{\phi}_{\rm DF} = 0$, and furthermore the priors of the environmental effects parameters $\boldsymbol{\theta}_{\rm env} = \left(\tilde{\phi}_{-4\rm PN}, \tilde{\phi}_{\rm DF}\right)$ and the other parameters $\boldsymbol{\theta}_{\rm vac} = (\chi_a, \chi_l, D_L, M_c, \eta, t_c, \iota, \lambda, \beta, \psi, \phi_c)$ are separable. Under these conditions, we could apply the Savage-Dickey method to calculate the Bayes factor.

Given that the basic model $M_{\rm env}$ is nested within the more complex model $M_{\rm MG+env}$, the evidence of the vacuum model $M_{\rm env}$ is equal to the evidence of the environment model $M_{\rm MG+env}$ when the dipole amplitude B is set to zero. This implies the equality of their evidences under that condition: $P(D|M_{\rm env}) = P(D|M_{\rm MG+env}, B = 0)$. Consequently, the Bayes factor in favour of the MG+environment model can be computed as the ratio of the posterior density to the prior density of the MG parameter B evaluated at zero within the broader model:

$$\mathcal{B}_{\rm vac} = \frac{P(D|M_{\rm vac})}{P(D|M_{\rm env})} = \left.\frac{P(\boldsymbol{\theta}_{\rm env}|D, M_{\rm env})}{\pi(\boldsymbol{\theta}_{\rm env}|M_{\rm env})}\right|_{\boldsymbol{\theta}_{\rm env}=0}. \tag{16}$$

$$\mathcal{B}^{\rm MG+env}_{\rm env} = \frac{P(D|M_{\rm MG+env})}{P(D|M_{\rm env})} = \frac{p(B = 0 \mid D, M_{\rm MG+env})}{\pi(B = 0 \mid M_{\rm MG+env})}. \tag{17}$$

In conclusion, employing the Savage-Dickey method, the assessment of the Bayes factor for two nested models necessitates solely the correctly normalized marginal posterior value at $\boldsymbol{\theta}_{\rm env} = 0$ under the environment model $M_{\rm env}$. This value is easily obtained from the MCMC PE results. In this research, we used the Kernel Density Estimation (KDE) method to approximate the distribution from the MCMC sampling points.

Therefore, the calculation requires only the marginalized posterior density of B at zero, which can be robustly estimated from the posterior samples obtained via standard Markov Chain Monte Carlo (MCMC) parameter estimation under model $M_{\rm MG+env}$. In this work, we apply Kernel Density Estimation (KDE) to the MCMC chains for the parameter B to accurately approximate $p(B = 0 \mid D, M_{\rm MG+env})$, thereby enabling a computationally efficient assessment of the evidence for the modified gravity effect beyond environmental explanations.

V. DATA SIMULATION AND RESULTS

In this work, since there is no actual detection data from space-borne GW detectors, we simulated the sBBH inspiral signals for TianQin. Meanwhile, as described in Subsec.III B, TianQin observation data compose of three channels (A,E,T). To access TianQin's capability to distinguish the environmental effects from data, we select the five-years observation time as per TianQin's design. During the observation period, as the "3 months on, 3 months off" observation schedule, we set the detector to operate in the 3rd∼6th, 9th∼12th, 15th∼18th, 21st∼24th, 27th∼30th, 33th∼36th, 39th∼42th, 45st∼48th, 51st∼54th, 57th∼60th month. Under these situations, the TianQin data is denoted as $D_{\rm TianQin}$: $[D_{3-6}, D_{9-12}, D_{15-18}, D_{21-24}, D_{27-30}, D_{33-36}, D_{39-42}, D_{45-48}, D_{51-54}, D_{57-60}]$. The total likelihood of these data segments can be expressed as,

$$\begin{aligned}\ln \mathcal{L}(D_{\rm TianQin}|\boldsymbol{\theta}) = &\ln \mathcal{L}(D_{0-3}|\boldsymbol{\theta}) + \ln \mathcal{L}(D_{6-9}|\boldsymbol{\theta}) \\ &+ \cdots + \ln \mathcal{L}(D_{57-60}|\boldsymbol{\theta}),\end{aligned} \tag{18}$$

Here we put a table with default GW190521-like system's parameter value.

TABLE I: Parameters of the GW190521

Parameters	**Symbols**	**GW190521-like**
Chirp mass ($M_\odot$)	M_c	77.66
Symmetric mass ratio	η	0.23
Primary spin, secondary spin	(χ_1, χ_2)	(0.8,0.8)
Inclination angle (rad)	ι	$\pi/6$
Luminosity distance(Mpc)	D_L	1000
Coalescence time(yrs)	t_c	5
Ecliptic longitude (rad)	λ	2.1
Ecliptic latitude angle (rad)	β	-0.082
Polarization angle (rad)	ψ	$\pi/4$
Coalescence phase (rad)	ϕ_c	0
Accretion+Acceleration	$\tilde{\phi}_{-4\mathrm{PN}}$	2.4×10^{-20}
Gas density (g/cm^3)	ρ	$[10^{-8}, 10^{-9}, 10^{-10}, 10^{-11}, 10^{-12}]$
Dipole radiation	B	4.4×10^{-5}

A. GW data simulation

Our data simulation is designed to generate the mock TianQin observations of a GW190521-like sBBH system, incorporating both environmental and modified gravity effects to assess their potential degeneracy. We adopt the intrinsic source component masses parameters from the GWTC-2 estimates for GW190521. And to explore a physically motivated range of environmental coupling, we vary the gas density parameter, which scales the magnitude of the -5.5PN environmental phase term, across values from 10^{-12} to 10^{-8} g/cm^3. This range is justified by standard thin-disk models of AGN accretion disks [93] surrounding central super mass black holes with masses between 10^6 and $10^9 M_\odot$ [94]. Furthermore, the chosen lower bound of 10^{-12} g/cm^3 is particularly relevant, as it close to the detectable threshold 10^{-11} g/cm^3 for constraining such environmental parameters with space-borne detectors over a multi-year observation timescale [32, 95, 96].

Besides, our simulation framework operates under three key assumptions to isolate the effect of interest. First, we model the TianQin noise as Gaussian and stationary. Second, we neglect systematic errors intrinsic to the vacuum waveform model to ensure any bias arises purely from the unmodeled environment. Third, we explicitly assume the sBBH inspirals within an AGN disk, providing the physical basis for the environmental modifications included in our signal model.

B. Parameter priors

To obtain the posterior of the parameters, one needs to specify the prior probability of all the parameters, and we adopt non-uniform priors for specific parameters and rest's prior distributions of all parameters are flat.

All the priors for the parameters are listed in the Table. II.

TABLE II: Priors of the GW events' parameters

Intrinsic	**Priors**	**Extrinsic**	**Priors**
M_c	$[0, 100]M_\odot$	D_L	$[0, 2000]$ Mpc
η	$[0.2, 0.25]$	Δt_c	$[-2000, +2000]$s
χ_a	$[-1, 1]$	λ	$[0, 2\pi]$
χ_l	$[-1, 1]$	$\sin\beta$	$[-1, 1]$
		$\cos\iota$	$[-1, 1]$
		ψ	$[0, \pi]$
		ϕ_c	$[0, 2\pi]$

C. Data analysis results

We present the parameter estimation results derived from analyzing the simulated TianQin data containing a single GW190521-like sBBH signal. The analysis aims to quantify how the presence of environmental effects biases the recovery of the dipole radiation parameter, B, and other source parameters.

Figure 1 presents the corner plot of the posterior probability distributions for key parameters, obtained from the analysis of a signal with an injected environmental gas density of $\rho_0 = 10^{-8}, \mathrm{g/cm}^3$. The plot illustrates both the one-dimensional marginalized posteriors and the two-dimensional correlations between parameters. In the top-left section of the corner plot, a strong negative correlation is observed between the effective spin parameters χ_a and χ_l. This degeneracy arises because, within the phase model of the `IMRPhenomD` waveform, these parameters appear in a combined product form; as linear combinations of the individual spin magnitudes χ_1 and χ_2, they cannot fully break the intrinsic degeneracy between the two component spins, consistent with our tests. Another notable correlation exists between the luminosity distance D_L and the inclination angle ι, as both parameters contribute primarily to the signal amplitude.

Notably, the dipole radiation parameter B is

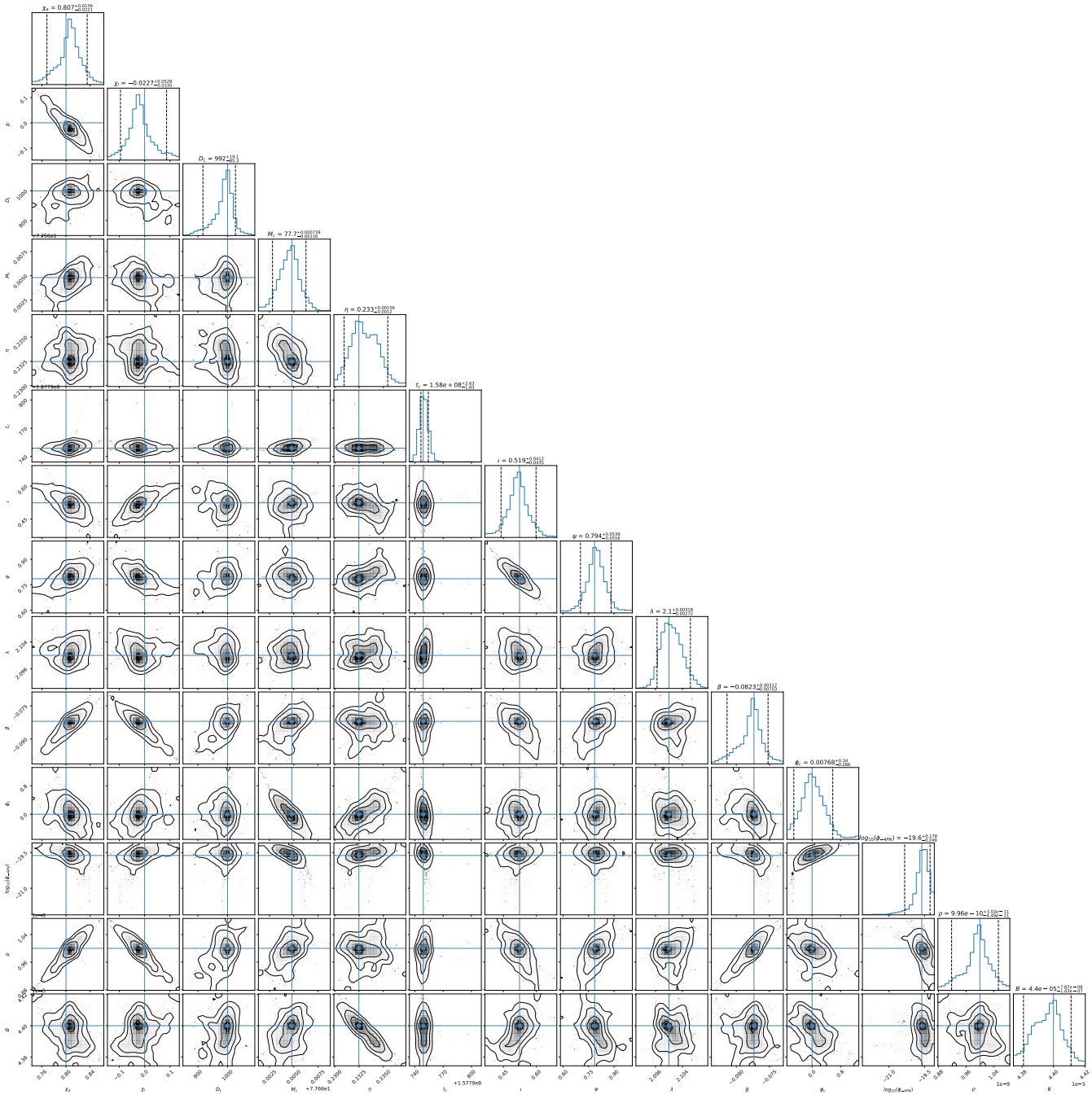

FIG. 1: The parameter estimation results of GW190521-like system. The black dashed lines indicate the GW waveform parameters' true values, and the $1-2\sigma$ contour plots represent the inferred PE results. The parameters of environmental effect on -4PN $\phi_{-4\mathrm{PN}}$ is changed into the logarithm form $\log_{10}(\phi_{-4\mathrm{PN}})$

.

well-constrained, with a recovered value of $B = 4.4 \times 10^{-5}{}^{+7.87\times10^{-8}}_{-1.03\times10^{-7}}$. The parameter estimation precision ΔB will close to 1% of the inject value. Furthermore, the PE results demonstrate that the parameter estimation precision of gas density $\Delta\rho \sim 10^{-11}\mathrm{g/cm}^{-3}$. The estimation precision ΔB reaches about 1% of the injected value. Furthermore, the parameter estimation precision for the gas density is $\Delta\rho \sim 10^{-11}\mathrm{g/cm}^{3}$. The high precision achieved in estimating both the environmental and dipole radiation parameters demonstrates the potential of space-borne gravitational-wave detectors to distinguish between these two effects in observational data. Using the Savage-Dickey method, a high Bayes factor $\mathcal{B}$ is expected, indicating that even in the presence of envi-

ronmental effects, the modified gravity signature (dipole radiation) is sufficiently pronounced to be robustly identified.

VI. CONCLUSION

In this work, we have systematically investigated the impact of AGN disk environmental effects on tests of gravitational dipole radiation using simulated stellar-mass binary black hole signals observed by TianQin. By constructing a waveform model that incorporates both parameterized environmental modifications (at -4PN order) and a -1PN dipole term, we performed comprehensive Bayesian parameter estimation and model selection on data containing both effects. Our analysis reveals a clear threshold: for gas densities above approximately $\rho_0 \sim 10^{-10}, \mathrm{g/cm}^3$, unmodeled environmental effects introduce significant bias into the inferred dipole parameter B and are strongly favoured by the data. Below this threshold, environmental contributions remain statistically negligible. These findings delineate the conditions under which future searches for beyond-GR physics with space-borne detectors must account for astrophysical environments to avoid systematic errors and false detections. This work provides a crucial reference for designing robust tests of general relativity in the era of space-based gravitational-wave astronomy.

Acknowledgments

Xiangyu thanks Jiandong Zhang and Jianwei Mei for their meaningful discussion of our work. This work has been supported by the National Key Research and Development Program of China (No. 2023YFC2206700), the Natural Science Foundation of China (Grant No. 12173104), the Natural Science Foundation of Guangdong Province of China (Grant No. 2022A1515011862), and the Fundamental Research Funds for the Central Universities, Sun Yat-sen University.

[1] B. P. Abbott et al. (LIGO Scientific, Virgo), Phys. Rev. X **9**, 031040 (2019), 1811.12907.
[2] R. Abbott et al. (LIGO Scientific, Virgo), Phys. Rev. X **11**, 021053 (2021), 2010.14527.
[3] R. Abbott et al. (LIGO Scientific, VIRGO) (2021), 2108.01045.
[4] R. Abbott et al. (KAGRA, VIRGO, LIGO Scientific), Phys. Rev. X **13**, 041039 (2023), 2111.03606.
[5] A. G. Abac et al. (LIGO Scientific, VIRGO, KAGRA) (2025), 2508.18082.
[6] B. P. Abbott et al. (LIGO Scientific, Virgo), Phys. Rev. D **100**, 104036 (2019), 1903.04467.
[7] R. Abbott et al. (LIGO Scientific, Virgo), Phys. Rev. D **103**, 122002 (2021), 2010.14529.
[8] R. Abbott et al. (LIGO Scientific, VIRGO, KAGRA), Phys. Rev. D **112**, 084080 (2025), 2112.06861.
[9] J. Luo et al. (TianQin), Class. Quant. Grav. **33**, 035010 (2016), 1512.02076.
[10] P. Amaro-Seoane et al. (LISA) (2017), 1702.00786.
[11] W.-R. Hu and Y.-L. Wu, Natl. Sci. Rev. **4**, 685 (2017).
[12] E. Berti, A. Buonanno, and C. M. Will, Phys. Rev. D **71**, 084025 (2005), gr-qc/0411129.
[13] A. Sesana, Phys. Rev. Lett. **116**, 231102 (2016), 1602.06951.
[14] S. Vitale, Physical Review Letters **117**, 051102 (2016), URL https://link.aps.org/doi/10.1103/PhysRevLett.117.051102.
[15] E. Barausse, N. Yunes, and K. Chamberlain, Phys. Rev. Lett. **116**, 241104 (2016), 1603.04075.
[16] C. Shi, M. Ji, J.-d. Zhang, and J. Mei (2022), 2210.13006.
[17] Z. Carson and K. Yagi, Class. Quant. Grav. **37**, 02LT01 (2020), 1905.13155.
[18] N. Cornish, L. Sampson, N. Yunes, and F. Pretorius, Phys. Rev. D **84**, 062003 (2011), URL https://link.aps.org/doi/10.1103/PhysRevD.84.062003.
[19] A. Toubiana, S. Marsat, E. Barausse, S. Babak, and J. Baker, Phys. Rev. D **101**, 104038 (2020), 2004.03626.
[20] I. Bartos, B. Kocsis, Z. Haiman, and S. Márka, Astrophys. J. **835**, 165 (2017), 1602.03831.
[21] N. C. Stone, B. D. Metzger, and Z. Haiman, Mon. Not. Roy. Astron. Soc. **464**, 946 (2017), 1602.04226.
[22] H. Tagawa, Z. Haiman, and B. Kocsis, Astrophys. J. **898**, 25 (2020), 1912.08218.
[23] H. Tagawa, B. Kocsis, Z. Haiman, I. Bartos, K. Omukai, and J. Samsing, Astrophys. J. **908**, 194 (2021), 2012.00011.
[24] V. Gayathri, Y. Yang, H. Tagawa, Z. Haiman, and I. Bartos, Astrophys. J. Lett. **920**, L42 (2021), 2104.10253.
[25] K. E. S. Ford and B. McKernan, Mon. Not. Roy. Astron. Soc. **517**, 5827 (2022), 2109.03212.
[26] J. Li, A. M. Dempsey, H. Li, D. Lai, and S. Li, Astrophys. J. Lett. **944**, L42 (2023).
[27] Y.-J. Li, Y.-Z. Wang, S.-P. Tang, and Y.-Z. Fan, Phys. Rev. Lett. **133**, 051401 (2024), URL https://link.aps.org/doi/10.1103/PhysRevLett.133.051401.
[28] Y.-J. Li, Y.-Z. Wang, S.-P. Tang, T. Chen, and Y.-Z. Fan, The Astrophys. J. **987**, 65 (2025), URL https://doi.org/10.3847/1538-4357/add535.
[29] Y.-J. Li, Y.-Z. Wang, S.-P. Tang, and Y.-Z. Fan (2025), 2509.23897.
[30] R. Abbott et al. (LIGO Scientific, Virgo), Phys. Rev. Lett. **125**, 101102 (2020), 2009.01075.
[31] M. J. Graham et al., Phys. Rev. Lett. **124**, 251102 (2020), 2006.14122.
[32] A. Caputo, L. Sberna, A. Toubiana, S. Babak, E. Barausse, S. Marsat, and P. Pani, Astrophys. J. **892**, 90 (2020), 2001.03620.
[33] A. Toubiana et al., Phys. Rev. Lett. **126**, 101105 (2021), 2010.06056.
[34] B. Kocsis, N. Yunes, and A. Loeb, Phys. Rev. D **84**, 024032 (2011), URL https://link.aps.org/doi/10.1103/PhysRevD.84.024032.

[35] C. Bonvin, C. Caprini, R. Sturani, and N. Tamanini, Phys. Rev. D **95**, 044029 (2017), URL https://link.aps.org/doi/10.1103/PhysRevD.95.044029.

[36] K. Inayoshi, N. Tamanini, C. Caprini, and Z. Haiman, Phys. Rev. D **96**, 063014 (2017), 1702.06529.

[37] N. Tamanini, C. Caprini, E. Barausse, A. Sesana, A. Klein, and A. Petiteau, JCAP **04**, 002 (2016), 1601.07112.

[38] S.-C. Yang, W.-B. Han, H. Tagawa, S. Li, Y. Jiang, P. Shen, Q. Yun, C. Zhang, and X.-Y. Zhong, Astrophys. J. Lett. **988**, L41 (2025), 2401.01743.

[39] E. Barausse, V. Cardoso, and P. Pani, Phys. Rev. D **89**, 104059 (2014), URL https://link.aps.org/doi/10.1103/PhysRevD.89.104059.

[40] L. Sberna et al., Phys. Rev. D **106**, 064056 (2022), 2205.08550.

[41] N. Yunes, B. Kocsis, A. Loeb, and Z. Haiman, Phys. Rev. Lett. **107**, 171103 (2011), 1103.4609.

[42] P. S. Cole, G. Bertone, A. Coogan, D. Gaggero, T. Karydas, B. J. Kavanagh, T. F. M. Spieksma, and G. M. Tomaselli, Nature Astron. **7**, 943 (2023), 2211.01362.

[43] A. M. Derdzinski, D. D'Orazio, P. Duffell, Z. Haiman, and A. MacFadyen, Mon. Not. Roy. Astron. Soc. **486**, 2754 (2019), [Erratum: Mon.Not.Roy.Astron.Soc. 489, 4860–4861 (2019)], 1810.03623.

[44] A. Derdzinski, D. D'Orazio, P. Duffell, Z. Haiman, and A. MacFadyen, Mon. Not. Roy. Astron. Soc. **501**, 3540 (2021), 2005.11333.

[45] G. Caneva Santoro, S. Roy, R. Vicente, M. Haney, O. J. Piccinni, W. Del Pozzo, and M. Martinez, Phys. Rev. Lett. **132**, 251401 (2024), 2309.05061.

[46] S. Kejriwal, L. Speri, and A. J. K. Chua, Phys. Rev. D **110**, 084060 (2024), 2312.13028.

[47] S. Y. Lau, K. Yagi, and P. Arras, Phys. Rev. D **111**, 024039 (2025), 2409.17418.

[48] M. Garg, L. Sberna, L. Speri, F. Duque, and J. Gair, Mon. Not. Roy. Astron. Soc. **535**, 3283 (2024), 2410.02910.

[49] E. C. Ostriker, Astrophys. J. **513**, 252 (1999), astro-ph/9810324.

[50] T. C. N. Boekholt, C. Rowan, and B. Kocsis, Mon. Not. Roy. Astron. Soc. **518**, 5653 (2023), 2203.09646.

[51] H. Tagawa, B. Kocsis, Z. Haiman, I. Bartos, K. Omukai, and J. Samsing, Astrophys. J. Lett. **907**, L20 (2021), 2010.10526.

[52] J. Miralda-Escude and A. Gould, Astrophys. J. **545**, 847 (2000), astro-ph/0003269.

[53] J. N. Bahcall and R. A. Wolf, Astrophys. J. **209**, 214 (1976).

[54] B. McKernan, K. E. S. Ford, W. Lyra, and H. B. Perets, Mon. Not. Roy. Astron. Soc. **425**, 460 (2012), 1206.2309.

[55] J. M. Bellovary, M.-M. Mac Low, B. McKernan, and K. E. S. Ford, Astrophys. J. Lett. **819**, L17 (2016), 1511.00005.

[56] A. Secunda, J. Bellovary, M.-M. Mac Low, K. E. Saavik Ford, B. McKernan, N. Leigh, W. Lyra, and Z. Sándor, Astrophys. J. **878**, 85 (2019), 1807.02859.

[57] R. Abbott et al. (LIGO Scientific, Virgo), Astrophys. J. Lett. **900**, L13 (2020), 2009.01190.

[58] Z. Barkat, G. Rakavy, and N. Sack, Phys. Rev. Lett. **18**, 379 (1967).

[59] S. E. Woosley, A. Heger, and T. A. Weaver, Reviews of Modern Physics **74**, 1015 (2002).

[60] J. Samsing, I. Bartos, D. J. D'Orazio, Z. Haiman, B. Kocsis, N. W. C. Leigh, B. Liu, M. E. Pessah, and H. Tagawa, Nature (London) **603**, 237 (2022), 2010.09765.

[61] N. Tamanini, A. Klein, C. Bonvin, E. Barausse, and C. Caprini, Phys. Rev. D **101**, 063002 (2020), URL https://link.aps.org/doi/10.1103/PhysRevD.101.063002.

[62] V. Cardoso and A. Maselli, Astron. Astrophys. **644**, A147 (2020), 1909.05870.

[63] B. P. Abbott et al. (LIGO Scientific, Virgo), Phys. Rev. Lett. **116**, 221101 (2016), [Erratum: Phys.Rev.Lett. 121, 129902 (2018)], 1602.03841.

[64] S. Liu, Y.-M. Hu, J.-d. Zhang, and J. Mei, Physical Review D **101**, 103027 (2020), publisher: American Physical Society.

[65] S. Khan, S. Husa, M. Hannam, F. Ohme, M. Pürrer, X. Jiménez Forteza, and A. Bohé, Phys. Rev. D **93**, 044007 (2016), 1508.07253.

[66] S. Husa, S. Khan, M. Hannam, M. Pürrer, F. Ohme, X. Jiménez Forteza, and A. Bohé, Phys. Rev. D **93**, 044006 (2016), 1508.07250.

[67] Y.-M. Hu, J. Mei, and J. Luo, Natl. Sci. Rev. **4**, 683 (2017).

[68] K. Beuermann, H. C. Thomas, K. Reinsch, A. D. Schwope, J. Trümper, and W. Voges, **347**, 47 (1999), ISSN 0004-6361, ADS Bibcode: 1999A&A...347...47B.

[69] G. L. Israel et al., Astron. Astrophys. **386**, L13 (2002), astro-ph/0203043.

[70] M. Tinto and J. W. Armstrong, Physical Review D **59**, 102003 (1999), publisher: American Physical Society.

[71] M. Vallisneri, Phys. Rev. D **71**, 022001 (2005), gr-qc/0407102.

[72] A. Krolak, M. Tinto, and M. Vallisneri, Phys. Rev. D **70**, 022003 (2004), [Erratum: Phys.Rev.D 76, 069901 (2007)], gr-qc/0401108.

[73] S. Marsat and J. G. Baker (2018), 1806.10734.

[74] S. Marsat, J. G. Baker, and T. Dal Canton, Phys. Rev. D **103**, 083011 (2021), 2003.00357.

[75] D. Foreman-Mackey, D. W. Hogg, D. Lang, and J. Goodman, Publ. Astron. Soc. Pac. **125**, 306 (2013), 1202.3665.

[76] J. Goodman and J. Weare, Commun. Appl. Math. Comput. Sc. **5**, 65 (2010).

[77] N. Leslie, L. Dai, and G. Pratten, Phys. Rev. D **104**, 123030 (2021), 2109.09872.

[78] X. Lyu, E.-K. Li, and Y.-M. Hu (2023), 2307.12244.

[79] A. Toubiana, S. Marsat, S. Babak, J. Baker, and T. Dal Canton, Phys. Rev. D **102**, 124037 (2020), 2007.08544.

[80] A. Toubiana, S. Babak, S. Marsat, and S. Ossokine, Phys. Rev. D **106**, 104034 (2022), 2206.12439.

[81] R. Buscicchio, A. Klein, E. Roebber, C. J. Moore, D. Gerosa, E. Finch, and A. Vecchio, Physical Review D **104**, 044065 (2021), ISSN 2470-0010, 2470-0029.

[82] N. J. Cornish, arXiv e-prints arXiv:1007.4820 (2010), 1007.4820.

[83] B. Zackay, L. Dai, and T. Venumadhav, arXiv e-prints arXiv:1806.08792 (2018), 1806.08792.

[84] M. L. Katz, Physical Review D **105**, 044055 (2022), 2111.01064.

[85] J. Skilling, Bayesian Analysis **1**, 833 (2006).

[86] J. M. Dickey and B. P. Lientz, Ann. Math. Statist. **41**, 214 (1970), URL https://doi.org/10.1214/aoms/1177697203.

[87] R. Trotta, Mon. Not. Roy. Astron. Soc. **378**, 72 (2007), astro-ph/0504022.

[88] C. Watkinson, A. R. Liddle, P. Mukherjee, and D. Parkinson, Mon. Not. Roy. Astron. Soc. **424**, 313 (2012), 1111.1870.
[89] R. L. Schuhmann, B. Joachimi, and H. V. Peiris, Mon. Not. Roy. Astron. Soc. **459**, 1916 (2016), 1510.00019.
[90] D. J. Reardon et al., Astrophys. J. Lett. **951**, L6 (2023), 2306.16215.
[91] C. J. Moore, E. Finch, A. Klein, V. Korol, N. Pham, and D. Robins, Mon. Not. Roy. Astron. Soc. **531**, 2817 (2024), 2310.06568.
[92] V. De Renzis, D. Gerosa, M. Mould, R. Buscicchio, and L. Zanga, Phys. Rev. D **108**, 024024 (2023), 2304.13063.
[93] E. Sirko and J. Goodman, Mon. Not. Roy. Astron. Soc. **341**, 501 (2003).
[94] D. Gangardt, A. A. Trani, C. Bonnerot, and D. Gerosa, Mon. Not. Roy. Astron. Soc. **530**, 3689 (2024), 2403.00060.
[95] P. Dutta Roy, P. Mahapatra, A. Samajdar, and K. G. Arun, Phys. Rev. D **111**, 104047 (2025).
[96] X. Lyu, E.-K. Li, C. Shi, and Y.-M. Hu (2025), 2511.10204.